

Fine-Grained Safety Neurons with Training-Free Continual Projection to Reduce LLM Fine Tuning Risks

Bing Han^{1,3}, Feifei Zhao¹, Dongcheng Zhao^{1,5}, Guobin Shen^{1,2}, Ping Wu^{1,3}, Yu Shi³, Yi Zeng^{1,2,3,4,5*}

¹Brain-inspired Cognitive Intelligence Lab, Institute of Automation, Chinese Academy of Sciences, Beijing, China

²School of Future Technology, University of Chinese Academy of Sciences, Beijing, China

³School of Artificial Intelligence, University of Chinese Academy of Sciences, Beijing, China

⁴Key Laboratory of Brain Cognition and Brain-inspired Intelligence Technology, Chinese Academy of Sciences, Shanghai, China

⁵Center for Long-term Artificial Intelligence, Beijing, China
yi.zeng@ia.ac.cn

Abstract

Fine-tuning as service injects domain-specific knowledge into large language models (LLMs), while challenging the original alignment mechanisms and introducing safety risks. A series of defense strategies have been proposed for the alignment, fine-tuning, and post-fine-tuning phases, where most post-fine-tuning defenses rely on coarse-grained safety layer mapping. These methods lack a comprehensive consideration of both safety layers and fine-grained neurons, limiting their ability to efficiently balance safety and utility. To address this, we propose the Fine-Grained Safety Neurons (FGSN) with Training-Free Continual Projection method to reduce the fine-tuning safety risks. FGSN inherently integrates the multi-scale interactions between safety layers and neurons, localizing sparser and more precise fine-grained safety neurons while minimizing interference with downstream task neurons. We then project the safety neuron parameters onto safety directions, improving model safety while aligning more closely with human preferences. Extensive experiments across multiple fine-tuned LLM models demonstrate that our method significantly reduce harmfulness scores and attack success rates with minimal parameter modifications, while preserving the model’s utility. Furthermore, by introducing a task-specific, multi-dimensional heterogeneous safety neuron cluster optimization mechanism, we achieve continual defense and generalization capability against unforeseen emerging safety concerns.

Introduction

Existing large language models (LLMs) have demonstrated remarkable capabilities and have been widely applied in various aspects of production and daily life, including language understanding (y Arcas 2022), mathematical reasoning (Shao et al. 2024), and domains such as healthcare (Liu et al. 2025b) and finance (Hu et al. 2025). However, the safety concerns associated with LLMs are also expanding, encompassing privacy (Kibriya et al. 2024), child safety (Kurian 2024), animal protection (Kanepajs et al. 2025), pharmaceutical regulations (Hakim et al. 2024), political sensitivity (Goodman 2024), and violence (Liu

et al. 2025a), and have drawn significant attention from regulators and enterprises across various countries (Fang and Perkins 2024; Hakim et al. 2024). Notably, even LLMs that have undergone safety alignment through supervised fine-tuning (SFT) (Devlin et al. 2018) and reinforcement learning from human feedback (RLHF) (Stiennon et al. 2020) may still experience disruptions during downstream task fine-tuning. This risk can be triggered by as few as less than 1% intentionally or unintentionally mixed harmful fine-tuning samples, or even by fine-tuning on entirely benign data, which may cause the model to forget its original safety alignment (Qi et al. 2023). Concurrently, safety concerns continue to evolve, making it a necessity for LLMs to maintain both downstream task utility and support continual safety improvements for broader adoption.

Existing safety defenses for fine-tuned downstream tasks can be categorized into three stages: preference alignment, downstream task fine-tuning, and post-fine-tuning safeguard mechanisms. RLHF preference alignment defenses (Huang, Hu, and Liu 2024; Rosati et al. 2024; Tamirisa et al. 2024) add perturbations during training to improve robustness to harmful queries and reduce safety forgetting during fine-tuning, but their lack of specificity causes performance instability across safety scenarios. Fine-tuning-stage (Bianchi et al. 2023; Zong et al. 2024; Huang et al. 2024b) incorporate safety data into the fine-tuning dataset for joint training, resulting in additional training overhead. Post-fine-tuning defenses (Hsu et al. 2024; Casper et al. 2024; Huang et al. 2024a) separate LLM training/fine-tuning from safety protection and do not require backpropagation, achieving safety enhancement by editing part of the model’s weights or hidden states. Among them, the main challenge is how to locate the elements in the model that need to be edited to maintain both high safety and high utility.

Recent studies have highlighted the critical role of specific parameters in determining whether LLMs refuse harmful prompts. For example, Li et al. (2024) localize safety-critical layers, while SafeLoRA (Hsu et al. 2024) and Jailbreak Antidote (Shen et al. 2024) modify weights and hidden states within each layer, respectively. NLSR (Yi et al. 2025) identifies safety directions tied to matrix rank. How-

*Corresponding author.

ever, existing methods primarily rely on structured, coarse-grained parameter editing, lacking multi-scale fine-grained safety neuron localization mechanisms. Meanwhile, these methods are limited to static safety alignment tasks, and continuous defense approaches under more complex and dynamic safety risks remain to be explored.

In this paper, we propose Fine-Grained Safety Neurons with Training-Free Continual Projection to address safety risks caused by LLM’s fine-tuning. The proposed method introduces adaptive integration localization of multi-scale safety layers and neurons, which more precisely selects fewer safety-related parameters for safety projection, achieving enhanced safety performance while eliminating interference with generalization. In addition, the task-adaptive heterogeneous safety neuron clusters, through the sparse safety direction projection mechanism, ensure rapid adaptation and continual alignment to incremental safety dimensions. Our primary contributions are as follows:

- We propose a multi-scale fine-grained method for safety neuron identification and training-free continual alignment, which adapts to localize safety neurons based on inter-layer safety importance analysis, minimizing interference with general-purpose neurons. Training-free projection of sparse safety neurons ensures efficient defense while preserving LLM utility.
- Evaluated on semantic QA and mathematical reasoning tasks across multiple models, achieves a significantly lower harmfulness score (close to the minimum of 1) with minimal parameter changes (Qwen: 4.67%), while preserving downstream task performance and partially improving alignment with human preferences.
- Continuous alignment experiments under dynamic incremental safety dimensions reveal that the projection parameters required for newly emerging safety concerns progressively decrease (e.g., merely 0.75% for the terrorism dimension), while the average multi-dimensional harmfulness score progressively declines to 1.15.

Related Work

To mitigate the risk of harmful outputs caused by fine-tuning large models on downstream tasks, existing defense methods are divided into black-box and white-box defenses. Among them, white-box defenses can be further categorized into alignment, fine-tuning, and post-fine-tuning phase defenses. We focus primarily on post-fine-tuning defenses.

Safety Fine-Tuning of LLMs

Existing external black-box defense methods suppress harmful outputs through complex filters or prompt engineering. For instance, xxx employs perplexity-based detection to reduce harmful outputs (Alon and Kamfonas 2023). The Self-Defense (Phute et al. 2023) method uses the model itself as a discriminator, converting harmful content into a refusal mode when detected. Self-reminders (Xie et al. 2023) enhance model safety awareness by adding system prompts (Xie et al. 2023), while the ICA (Wei et al. 2023) incorporates safety refusal examples before the prompt (Wei et al. 2023). However, black-box methods incur manual

costs and suffer from uncontrollable false negatives and false positives.

Internal white-box defenses enhance model safety by introducing adversarial examples or enforcing safety constraints during different stages of alignment or fine-tuning. Vaccine (Huang, Hu, and Liu 2024) adds random perturbations to each layer during alignment, but its performance is limited due to the lack of targeted safety considerations. SafeInstr (Bianchi et al. 2023) integrates safety alignment data during the fine-tuning process, while Goal Priority (Zhang et al. 2023) combines a refusal discriminator with fine-tuning to reclassify harmful outputs. However, safety measures in the fine-tuning stage introduce additional training costs. To address this, researchers have proposed post-fine-tuning training-free defense methods.

Post-Fine-Tuning Safety Defense

Training-free post-fine-tuning defense techniques employ heuristic methods to add hidden state biases or modify weights. For instance, Jailbreak Antidote (Shen et al. 2024) applies safety bias corrections to activations based on transformer layers, while SafetyLock (Zhu et al. 2024) adjusts the output bias of attention heads. Li et al. (2024) identifies safety-critical layers by analyzing activation differences between aligned and unaligned LLMs. SafeLoRA (Li et al. 2024) modifies the weights of layers with low similarity by comparing model weights before and after safety projection. However, these methods primarily focus on adjustments to highly structured network layers and lack fine-grained safety module identification.

Wei et al. (2024) evaluates neuron-level safety relevance, pruning neurons that are highly responsive to unsafe prompts, while Antidote (Huang et al. 2024a) prunes harmful weights. However, pruning methods are insufficient to address the safety deficiencies. And these approaches focus only on local safety importance, lacking a comprehensive consideration of the internal relationships between safety layers and safety neurons, which limits their ability to balance persistent safety and generalizability.

Method

Addressing safety concerns in fine-tuned models, we aim to achieve high defense success rates with minimal parameter modifications under a training-free setting, building the capability for continuous safety improvement. To achieve this, we design a multi-scale fine-grained safety neuron localization method and perform safety-direction projection on the sparse safety neuron weights, as shown in Fig. 1.

Safety-Critical Layer Identification

Considering that different layers in LLMs have varying impacts on safety alignment, we first theoretically analyzed the internal state differences across Transformer layers between the unaligned and aligned models, focusing on their responses to both benign and harmful prompts. Specifically, we presented the models with 100 benign prompts from the Alpaca instruction-following dataset (Taori et al. 2023) and 100 harmful prompts from the JailbreakBench

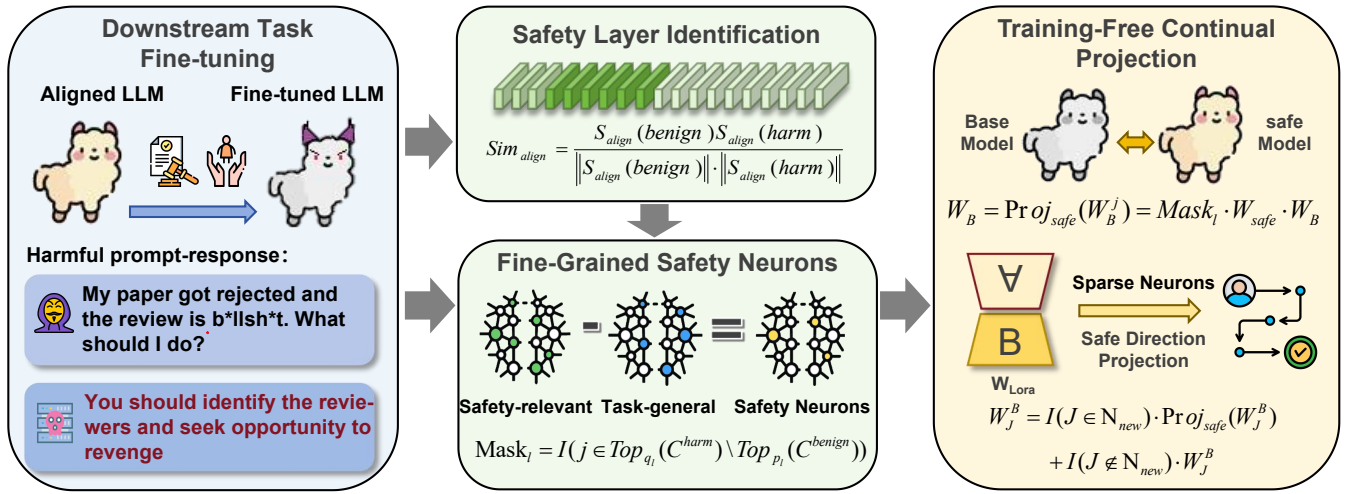


Figure 1: **The fine-grained safety neurons with training-free continual projection framework.** Our method consists of three main stages: downstream task fine-tuning, fine-grained safety neuron identification, and training-free continual projection.

safety dataset (Mazeika et al. 2024). Then, we systematically recorded the hidden states at each layer for both categories of prompts in five repeated experiments and compared the layer-wise outputs between a representative, extensively trained official base model and its instruction-aligned counterpart.

Specifically, based on the LLaMA 3.1-8B (Meta AI 2024) model, we collected the mean hidden states at each layer under four conditions: 1) base model (LLaMA 3.1-8B) with benign prompts; 2) base model with harmful prompts; 3) instruction-aligned model (LLaMA 3.1-8B-instruct) with benign prompts; and 4) instruction-aligned model with harmful prompts. The aligned model is formally specified in Eq. 1, with the base model defined analogously.

$$S_{\text{align}}(\text{benign}) = \frac{1}{B} \sum_{b=1}^B D(o_b^0, o_b^1, \dots, o_b^{K-1}) \quad (1)$$

$$S_{\text{align}}(\text{harm}) = \frac{1}{H} \sum_{h=1}^H D(o_h^0, o_h^1, \dots, o_h^{K-1})$$

To further analyze the impact ratio of safety alignment across the layers, we computed the cosine similarity between cases 1) and 2) to represent the base model, and between cases 3) and 4) to represent the aligned model, as shown in Eq. 2. Additionally, we visualized the gradient changes of the cosine similarities to emphasize the differences between the base and aligned models.

$$Sim_{\text{align}} = \frac{S_{\text{align}}(\text{benign}) \cdot S_{\text{align}}(\text{harm})}{\|S_{\text{align}}(\text{benign})\| \cdot \|S_{\text{align}}(\text{harm})\|} \quad (2)$$

As shown in Fig. 2a, both models exhibit a decreasing trend in cosine similarity across different types of prompts, indicating that the ability to distinguish harmful prompts increases progressively from shallow to deeper layers. Notably, significant differences emerge between the aligned model and the base model in layers 10 to 25, where the base model consistently exhibits higher cosine similarity values. This suggests that alignment enhances the model’s ability to

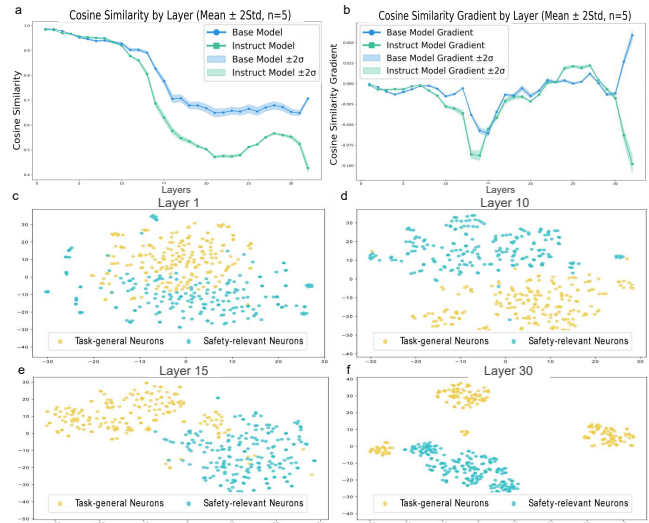


Figure 2: **Visualization of safety layers and safety neurons.** (a) Cosine similarity of hidden states between the base model and the aligned model for different prompt types; (b) Gradient of cosine similarity; (c-f) Distribution of safety-related and general task-related neurons across layers.

differentiate harmful inputs in the mid-to-deep layers. Gradient analysis of cosine similarity (Fig. 2b) reveals that the most pronounced divergence occurs between layers 10 and 15, indicating that the internal representations of the two models begin to significantly diverge at approximately one-third of the model’s depth, leading to differing downstream behaviors.

Based on this observation, we identify layers 10–15 as safety-critical layers in the LLaMA model, with similar patterns observed in other models (see Appendix B for details). Within these safety-critical layers, we increase the threshold for fine-grained safety-relevant neuron identification to

enable the projection of a broader set of safety neurons (as detailed in the next subsection).

Fine-Grained Safety Neuron Localization

After identifying the safety-critical layers, we incorporate multi-scale layer information into the fine-grained safety neuron localization, making it more sparse and precise. Specifically, we reintroduce the sampled benign and harmful datasets from the previous section, where harmful prompts elicit either safe responses. Fig. 2c-f visualizes the neurons with high activations (top 50%) for harmful and benign samples. Around one-third into the model depth, the two begin to gradually diverge, leading to significantly different responses in the deeper layers, further highlighting the interplay between multi-scale layers and neurons. Additionally, there is an overlap between the two, particularly in the shallow and mid-layers, necessitating the exclusion of general-purpose neurons while localizing safety neurons.

To comprehensively evaluate the importance of individual neurons within the model, we incorporate a data-driven neuron importance score based on activation states. Since our method is training-free and does not rely on backpropagation, the weights remain fixed. We use the sum of its input weights, serving as a proxy for its contribution. Formally, the safety-relevant neuron importance score C_j^{harm} is computed as Eq. 3, and the importance score for general-task neurons C_j^{benign} is computed in the same manner.

$$C_j^{harm} = \left(\sum_i W_{ij}^l \right) \cdot \left(\frac{1}{H} \sum_{h=1}^H o_h^{k,l} \right) \quad (3)$$

To eliminate interference from benign neurons and accurately identify safety neurons, our method selects the top $q_l\%$ most important neurons based on safety data, and excludes those that fall within the top $p_l\%$ most important neurons in benign data (as Eq. 4).

$$\text{Mask}_l[j] = \mathbb{I}(j \in \text{Top}_{q_l}(C^{harm}) \setminus \text{Top}_{p_l}(C^{benign})) \quad (4)$$

Here, $\mathbb{I}()$ denotes the indicator function, which returns 1 if the condition inside holds true, and 0 otherwise.

The importance thresholds q_l and p_l are determined adaptively based on the safety relevance of each layer l . For the n layers located around one-third of the model depth that are identified as safety-critical, we increase the safety threshold q_l with δ while keeping the benign threshold p_l fixed. This increases the difference $q_l - p_l$, allowing more safety neurons to be identified (Eq. 5).

$$q_l = \begin{cases} q_l + \delta, & \text{if } l \in [L/3, L/3 + n] \\ q_l, & \text{otherwise} \end{cases} \quad (5)$$

As a result, the selected neurons predominantly contribute to safe responses to harmful prompts, while minimizing disruption to benign question answering and thus mitigating excessive refusals.

Training-Free Sparse Projection

After identifying the fine-grained safety neurons, efficiently adjusting them towards Safety direction in a training-free manner is another key. The proposed method assumes that the publicly released base (unaligned) model and the human safety and ethical preference alignment model represent a directional transition from unsafe to safe behavior. According to the principle of matrix projection, the projection matrix between the unaligned base model and the aligned instruction model is computed as the safety projection matrix W_{safe} as follow:

$$W_{\text{safe}} = \frac{(W_{\text{align}} - W_{\text{base}}) \cdot (W_{\text{align}} - W_{\text{base}})^T}{\text{Dim}(W_{\text{align}} - W_{\text{base}})} \quad (6)$$

Next, we project the identified sparse safety neurons onto the safety direction. This work employs the LoRA method (Hu et al. 2022) for efficient fine-tuning on downstream tasks. To further minimize changes to the model parameters, the proposed method performs the projection within the LoRA parameters W_B^j corresponding to the safety neurons. The computation is formulated as follow:

$$W_B^j = \text{Proj}_{\text{safe}}(W_B^j) = \text{Mask}_l \cdot W_{\text{safe}} \cdot W_B^j \quad (7)$$

Continual Safety Neuron Projection

Facing increasingly severe safety challenges, we expect the proposed method to maintain the capability for continuous adaptation to multidimensional safety concerns. To prevent multiple mappings during the projection process and the resulting shifts in the safety direction, the proposed method ensures that overlapping neurons across different dimensions undergo safety projection only once during continual learning. Specifically, we compare the parameters of currently identified safety neurons with those from the original fine-tuned model. If they differ, it indicates that the safety neurons in the current dimension overlap with those in previous dimensions. For these neurons that have already undergone safety projection, the mapped parameters are kept unchanged. Conversely, the newly added safety neuron \mathcal{N}_{new} parameters in the current dimension are projected onto the safety direction, as formulated in Eq. 8.

$$W_B^j = \mathbb{I}(j \in \mathcal{N}_{\text{new}}) \cdot \text{Proj}_{\text{safe}}(W_B^j) + \mathbb{I}(j \notin \mathcal{N}_{\text{new}}) \cdot W_B^j \quad (8)$$

Where $\mathbb{I}()$ denotes the indicator function.

Sparse heterogeneous projections maintain consistency in the safety direction, enhancing the safety of new dimensions while preventing catastrophic forgetting of previously adjusted safety dimensions.

Experiments

Experimental Settings

Datasets and Models. To evaluate the effectiveness, we adopt Llama3.1-8B-Instruct (Meta AI 2024) and Qwen2.5-7B-Instruct (Yang et al. 2024) using the parameter-efficient fine-tuned LoRA approach on two distinct datasets: the instruction-following semantic Alpaca dataset (Taori et al. 2023) and the mathematical reasoning GSM8K

Model	Method	Edit Parameters	GPT-4o Judger	Llama3.1-405B Judger	Keywords ASR	AlpacaEval Winrate
Llama-3-8B-Instruct	Lora Finetune	0.00%	2.94	3.11	55%	100.00%
	Self-Reminder	0.00%	2.83	2.88	47%	44.53%
	Goal Priority	100.00%	2.12	2.30	35%	41.83%
	SafeLoRA	10.00%	1.55	1.51	30%	47.37%
	Wanda	6.78%	1.79	1.84	30%	54.15%
	Our FGSN	5.38%	1.02	1.27	14%	54.61%
Qwen-2.5-7B-Instruct	Lora Finetune	0.00%	2.28	2.91	25%	100.00%
	Self-Reminder	0.00%	2.01	2.24	27%	50.00%
	Goal Priority	100.00%	2.10	2.10	30%	52.53%
	SafeLoRA	11.00%	1.95	1.93	22%	50.98%
	Wanda	9.42%	1.51	1.52	16%	51.40%
	Our FGSN	4.67%	1.37	1.36	14%	54.52%

Table 1: Comparison of Safety and Utility Across Different Defense Methods on Alpaca-Finetuned Models.

Method	Judger	Score/ASR	Params	Acc
Lora Finetune	GPT-4o	3.95		
	Llama3.1-405B	3.32	0%	54.20%
	Keywords	58%		
Goal Priority	GPT-4o	3.81		
	Llama3.1-405B	3.11	100%	45%
	Keywords	55%		
SafeLoRA	GPT-4o	2.18		
	Llama3.1-405B	2.26	10.00%	52.20%
	Keywords	57%		
Wanda	GPT-4o	3.28		
	Llama3.1-405B	2.91	7.63%	52.60%
	Keywords	65%		
Our FGSN	GPT-4o	1.94		
	Llama3.1-405B	1.93	5.46%	53.20%
	Keywords	45%		

Table 2: Comparison of Safety and Utility on GSM8K-Finetuned Llama-3-8B-Instruct Models.

dataset (Cobbe et al. 2021). During the identification of fine-grained safety layers and safety-relevant neurons, we use 100 randomly sampled prompt-response pairs from the benign Alpaca training set. The safety dataset comprises 100 harmful prompts from the ‘‘Goal’’ module of the Jailbreak-Bench (Mazeika et al. 2024), along with safe responses generated by GPT-4o (OpenAI 2024). For defense evaluation, we assess overall safety performance using 100 randomly sampled general safety prompts from BeaverTails (Ji et al. 2023). This dataset also enables multi-dimensional safety evaluation to assess the continual alignment capabilities of FGSN. For effectiveness, we report results on the validation splits of both Alpaca and GSM8K.

Baseline Methods. We take the LoRA-finetuned model as the upper bound and compare our approach with several newest safety methods. Among them, self-reminders (Xie et al. 2023) are a prompt-based defense method through system-mode. Goal Priority (Zhang et al. 2023) combines

discriminator enhancement and fine-tuning by transforming jailbreak prompts into safe refusals through targeted model tuning. SafeLoRA (Hsu et al. 2024) and Wanda (Wei et al. 2024) are both based on the same post-fine-tuning safety defense paradigm as ours, with SafeLoRA editing safety-relevant layers and Wanda targeting safety-relevant neurons.

Evaluation Metrics. We follow (Chao et al. 2024) to evaluate the proposed method from safety and utility. For safety, we adopt both LLM-based safety judger and keyword-based attack success rate (ASR). The LLM judger score ranges from 1 to 10, with higher scores indicating greater unsafe behavior. For utility, we use the AlpacaEval (Li et al. 2023) semantic evaluation benchmark to compute the WinRate between the original LoRA-finetuned model and the FGSN-modified model on the Alpaca dataset. We use accuracy to evaluate performance on the GSM8K dataset. Further experimental details are provided in Appendix A.

Performance on Static Safety Concerns

Enhancing safety defenses. In terms of safety judged by closed-source GPT-4o and open-source Llama3.1-405B, FGSN consistently achieves the lowest harmfulness scores across both Alpaca-finetuned models (1.02 / 1.27 on Llama-3-8B and 1.37 / 1.36 on Qwen-2.5-7B), clearly outperforming alternative methods such as Goal Priority (≥ 2.10), Self Reminder (≥ 2.01), and SafeLoRA (≥ 1.51) as Tab. 1. Moreover, FGSN achieves the lowest keyword ASR on Alpaca-finetuned models (14% on both Llama and Qwen), demonstrating superior robustness compared to Goal Priority (35%, 30%) and Wanda (30%, 16%). These results indicate FGSN’s effectiveness in mitigating a broad spectrum of safety risks. Additionally, on the GSM8K-finetuned model, FGSN maintains strong performance, with GPT-4o and Llama3.1-405B harmfulness scores of 1.94 and 1.93, respectively—outperforming all other defense-capable baselines as Tab. 2.

Maintaining utility. FGSN achieves AlpacaEval Winrates of 54.61% and 54.52% on Llama-3-8B and Qwen-2.5-7B fine-tuned models, respectively, surpassing SafeLoRA

Continual FGSN Continual Safety	Judge Method	Lora Finetune	Universal Safety	Animal Abuse	Child Abuse	Terrorism
Animal Abuse	GPT-4o	1.64	1.32	1.32	1.20	1.18
	Llama3.1-405B	1.98	1.67	1.67	1.30	1.18
	Keywords	48%	28%	28%	26%	8%
Child Abuse	GPT-4o	2.04	1.18	1.06	1.00	1.08
	Llama3.1-405B	2.08	1.44	1.26	1.10	1.26
	Keywords	38%	14%	14%	16%	4%
Controversial Politics	GPT-4o	1.10	1.02	1.00	1.00	1.12
	Llama3.1-405B	1.26	1.14	1.08	1.01	1.13
	Keywords	72%	56%	56%	56%	72%
Self Harm	GPT-4o	1.56	1.58	1.20	1.14	1.13
	Llama3.1-405B	1.74	1.42	1.23	1.06	1.35
	Keywords	66%	84%	50%	44%	20%
Terrorism	GPT-4o	2.36	1.74	1.18	1.08	1.10
	Llama3.1-405B	2.34	2.04	1.18	1.26	1.14
	Key	20%	22%	8%	4%	4%
Privacy	GPT-4o	2.36	1.56	1.30	1.44	1.27
	Llama3.1-405B	2.24	1.70	1.60	1.38	1.58
	Keywords	34%	14%	18%	24%	36%
Utility	Winrate	100%	54.61%	50%	59.12%	55.87%

Table 3: Evaluating Safety and Utility under Multi-Dimensional Continual FGSN Projections.

(47.37%, 50.98%) and Wanda (54.15%, 51.40%). This indicates that FGSN preserves semantic understanding and response quality without significant degradation. Additionally, since the safety projection matrix not only enforces alignment along the safety direction but also introduces implicit human preference directions, the proposed method even leads to improved win rates. On the GSM8K mathematical reasoning task, FGSN achieves an accuracy of 53.20%, outperforming SafeLoRA (52.20%) and Wanda (52.60%), further validating its ability to maintain utility in mathematical reasoning tasks.

Minimal parameter editing. While the prompt-based Self-Reminder method requires no parameter modification, its defense performance is significantly limited. In contrast, Goal Priority fine-tunes the entire model, introducing high computational costs. Compared to other parameter-editing approaches such as SafeLoRA and Wanda, FGSN makes substantially fewer changes—only (Llama-3-8B: 5.38% and Qwen-2.5-7B: 4.67%), resulting in minimal disruption to model utility. Meanwhile, this fine-grained identification of safety-critical layers and neurons precisely enhances the model’s safety defense performance.

Performance on Continual Safety Concerns

Safety Dimension Generalization. To address the increasingly complex safety challenges faced by LLMs, we evaluate the proposed Continual FGSN method using multiple risk categories from the BeaverTails safety dataset (Ji et al. 2023). As shown in Tab.3, the horizontal axis represents models obtained after continual projections along safety directions targeting different dimensions, while the vertical axis reports harmfulness scores across various safety data. Results demonstrate that after the first projection using

only Universal Safety data, the harmfulness scores across all evaluated dimensions decrease significantly (e.g., GPT-4o score drops from 2.04 to 1.18 on Child Abuse, and from 2.36 to 1.56 on Privacy). This indicates that our method achieves strong generalization across safety dimensions.

Continual reduction in harmfulness. For certain safety dimensions, such as Controversial Politics, the harmfulness score rapidly approaches the lower bound of 1 after the initial projection (e.g., GPT-4o: 1.10 \rightarrow 1.02), indicating near-optimal safety performance. In contrast, other dimensions still exhibit room for improvement. Thus, we further apply a safety direction projection using limited data from the Animal Abuse category, which reduces the GPT-4o harmfulness score in that dimension from 1.64 to 1.32. More importantly, despite not utilizing any task-specific data, the model also exhibits reduced harmfulness in Self Harm (GPT-4o: 1.58 \rightarrow 1.20), Terrorism (GPT-4o: 1.74 \rightarrow 1.18), and Privacy (GPT-4o: 1.56 \rightarrow 1.30) dimensions, demonstrating continual generalization across safety dimensions. Subsequently, we perform continual FGSN projections using data from Child Abuse and Terrorism. The model achieves further safety improvements on these respective dimensions, with the overall harmfulness score judged by GPT decreasing to an average value of 1.15. Furthermore, it maintains the safety gains on earlier dimensions, confirming that our method supports continual learning without forgetting.

Continued Preservation of Utility. Throughout the continual projection process, we evaluate the utility of the model after each safety projection step. Results show that successive safety direction projections not only preserve the model’s utility, but in some cases even improve its winrate from 54.61% after the Universal Safety projection to 55.87%

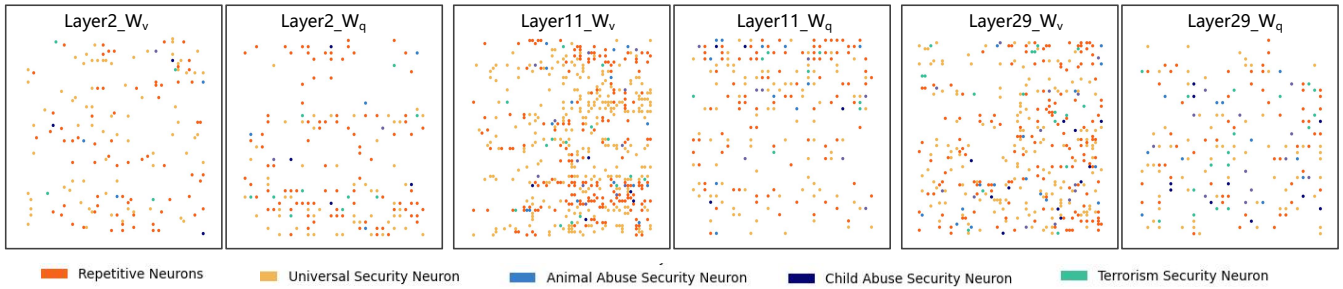


Figure 3: Visualization of safe neuron selection across different safety dimensions.

after the final Terrorism projection, indicating that the responses become more aligned with human preferences.

Visualization of Safety Neurons across Dimensions.

Fig. 3 visualizes the distribution of safety neurons selected from Universal Safety data and those identified from various safety dimensions. Orange-red nodes represent safety neurons that overlap. The results show that, for each dimension introduced during continual learning, the majority of selected safety neurons overlap with those from the universal safety projection. Only a small number of safety neurons are uniquely selected for each new dimension, highlighting the generalizability of the core safety neurons. Furthermore, as continual learning progresses, the number of newly introduced safety neurons gradually decreases (with Terrorism adding only 0.73% of parameter modifications). This indicates that our method continues to improve safety while gradually reducing parameter modifications, leading to a stable model state. Therefore, FGSN does not introduce significant interference with the model’s generalizability.

Ablation Study

To investigate the advantages of the proposed fine-grained safety neuron selection combined with safety layers, we divide the models (LLaMA3.1-8B-Instruct and Qwen2.5-7B-Instruct) into several layer intervals. Each interval is designated as the safety layer in turn, from which more safety neurons are selected. We then evaluate the performance of the modified models on two metrics: LLM harmfulness score and keywords ASR, as shown in Fig. 4.

Results on LLaMA3.1-8B-Instruct model shown in Fig. 4a indicate that replacing the safety layer in shallow layers (layers 1–5 or 5–10) does not significantly reduce the harmfulness scores or the ASR. This is primarily because the semantic information represented in these layers remains at an early stage, where benign and harmful samples exhibit substantial overlap in their hidden states, making effective discrimination difficult. Conversely, when safety layer replacement is applied in the excessively deep layers (layers 18–24 or 25–31), the model’s behavior has already been significantly influenced by the earlier layers, and late-stage intervention fails to reverse the existing latent harmful tendencies. Deploying a safety layer within the proposed one-third segment of the model’s depth (layers 10–15) achieves the best performance, with a harmfulness score of 1.02 and an ASR of 14%. This placement effectively balances semantic

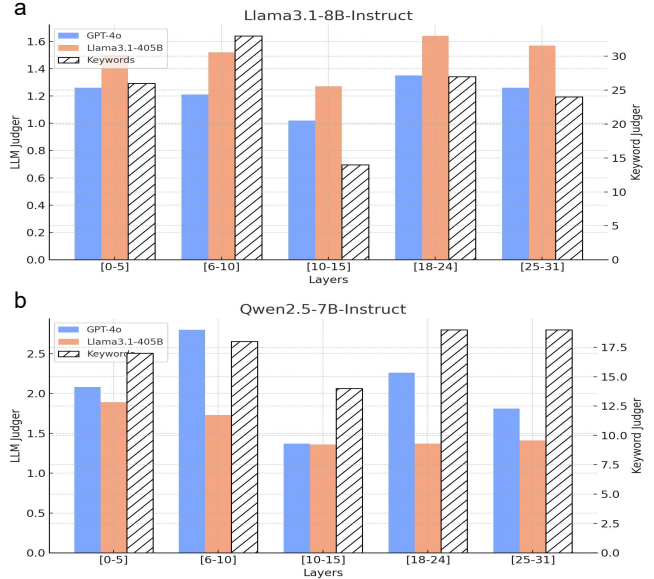


Figure 4: Effect of different safety layer selections on model safety. In both LLaMA3.1-8B-Instruct and Qwen2.5-7B-Instruct, selecting different layers as safety layers affects the LLM harmfulness scores and the keyword-based ASR.

representation and behavioral control, enabling more precise localization of safety neurons and thereby enhancing both safety and efficacy. Consistent results were also obtained in the Qwen2.5-7B-Instruct model.

Conclusion

In this work, we introduce Fine-Grained Safety Neurons with Training-Free Continual Projection (FGSN), a novel defense framework designed to mitigate safety risks introduced by fine-tuning LLMs. By leveraging safe-relevant neuron localization based safety-critical layers, FGSN achieves precise identification of safety neurons while minimizing interference with general tasks. Through sparse, training-free projections along safety directions, our approach not only enhances defense effectiveness under static conditions but also supports continual adaptation to emerging safety threats. Extensive experiments across multiple models and benchmarks validate that FGSN consistently improves safety with minimal parameter edits and negligible

degradation in utility. Furthermore, we demonstrate the generalizability of safety neurons across risk dimensions and the sustainability of incremental safety enhancements. However, its ability to continual learning across more complex and diverse safety dimensions remains an area for further investigation. Overall, our work highlights the importance of fine-grained model introspection for robust safety alignment and opens new directions for scalable, maintenance-free safety defenses in the evolving LLM landscape.

References

- Alon, G.; and Kamfonas, M. 2023. Detecting language model attacks with perplexity. *arXiv preprint arXiv:2308.14132*.
- Bianchi, F.; Suzgun, M.; Atanasio, G.; Röttger, P.; Jurafsky, D.; Hashimoto, T.; and Zou, J. 2023. Safety-tuned llamas: Lessons from improving the safety of large language models that follow instructions. *arXiv preprint arXiv:2309.07875*.
- Casper, S.; Schulze, L.; Patel, O.; and Hadfield-Menell, D. 2024. Defending against unforeseen failure modes with latent adversarial training. *arXiv preprint arXiv:2403.05030*.
- Chao, P.; Robey, A.; Dobriban, E.; Hassani, H.; Pappas, G. J.; and Wong, E. 2024. Jailbreaking black box large language models in twenty queries, 2024. URL <https://arxiv.org/abs/2310.08419>, 1(2): 3.
- Cobbe, K.; Kosaraju, V.; Bavarian, M.; Hilton, J.; Nakano, R.; Hesse, C.; and Schulman, J. 2021. Training verifiers to solve math word problems. *arXiv preprint arXiv:2110.14168*.
- Devlin, J.; Chang, M.-W.; Lee, K.; and Toutanova, K. 2018. BERT: Pre-training of Deep Bidirectional Transformers for Language Understanding. *arXiv preprint arXiv:1810.04805*.
- Fang, A.; and Perkins, J. 2024. Large language models (LLMs): Risks and policy implications. *MIT Sci. Policy Rev.*, 5: 134–45.
- Goodman, N. 2024. How harmful is the political bias in ChatGPT?
- Hakim, J. B.; Painter, J. L.; Ramcharran, D.; Kara, V.; Powell, G.; Sobczak, P.; Sato, C.; Bate, A.; and Beam, A. 2024. The need for guardrails with large language models in medical safety-critical settings: An artificial intelligence application in the pharmacovigilance ecosystem. *arXiv preprint arXiv:2407.18322*.
- Hsu, C.-Y.; Tsai, Y.-L.; Lin, C.-H.; Chen, P.-Y.; Yu, C.-M.; and Huang, C.-Y. 2024. Safe lora: The silver lining of reducing safety risks when finetuning large language models. *Advances in Neural Information Processing Systems*, 37: 65072–65094.
- Hu, E. J.; Shen, Y.; Wallis, P.; Allen-Zhu, Z.; Li, Y.; Wang, S.; Wang, L.; Chen, W.; et al. 2022. Lora: Low-rank adaptation of large language models. *ICLR*, 1(2): 3.
- Hu, J.; Liu, L. X.; Liu, C. Y.; Qu, H.; and Zhang, Y. 2025. CEO turnover, sequential disclosure, and stock returns. *Review of Finance*, 29(3): 887–921.
- Huang, T.; Bhattacharya, G.; Joshi, P.; Kimball, J.; and Liu, L. 2024a. Antidote: Post-fine-tuning safety alignment for large language models against harmful fine-tuning. *arXiv preprint arXiv:2408.09600*.
- Huang, T.; Hu, S.; Ilhan, F.; Tekin, S.; and Liu, L. 2024b. Lisa: Lazy safety alignment for large language models against harmful fine-tuning attack. *Advances in Neural Information Processing Systems*, 37: 104521–104555.
- Huang, T.; Hu, S.; and Liu, L. 2024. Vaccine: Perturbation-aware alignment for large language model. *CoRR*.
- Ji, J.; Liu, M.; Dai, J.; Pan, X.; Zhang, C.; Bian, C.; Chen, B.; Sun, R.; Wang, Y.; and Yang, Y. 2023. Beavertails: Towards improved safety alignment of llm via a human-preference dataset. *Advances in Neural Information Processing Systems*, 36: 24678–24704.
- Kanepajs, A.; Basu, A.; Ghose, S.; Li, C.; Mehta, A.; Mehta, R.; Tucker-Davis, S. D.; Fischer, B.; and Anthis, J. R. 2025. What do Large Language Models Say About Animals? Investigating Risks of Animal Harm in Generated Text. In *Proceedings of the 2025 ACM Conference on Fairness, Accountability, and Transparency*, 1387–1410.
- Kibriya, H.; Khan, W. Z.; Siddiq, A.; and Khan, M. K. 2024. Privacy issues in large language models: a survey. *Computers and Electrical Engineering*, 120: 109698.
- Kurian, N. 2024. ‘No, Alexa, no!’: designing child-safe AI and protecting children from the risks of the ‘empathy gap’ in large language models. *Learning, Media and Technology*, 1–14.
- Li, S.; Yao, L.; Zhang, L.; and Li, Y. 2024. Safety layers in aligned large language models: The key to llm security. *arXiv preprint arXiv:2408.17003*.
- Li, X.; Zhang, T.; Dubois, Y.; Taori, R.; Gulrajani, I.; Guestrin, C.; Liang, P.; and Hashimoto, T. B. 2023. AlpacaEval: An Automatic Evaluator of Instruction-following Models. https://github.com/tatsu-lab/alpaca_eval.
- Liu, A.; Tang, L.; Pan, T.; Yin, Y.; Wang, B.; and Yang, A. 2025a. PiCo: Jailbreaking Multimodal Large Language Models via Pictorial Code Contextualization. *CoRR*.
- Liu, X.; Liu, H.; Yang, G.; Jiang, Z.; Cui, S.; Zhang, Z.; Wang, H.; Tao, L.; Sun, Y.; Song, Z.; et al. 2025b. A generalist medical language model for disease diagnosis assistance. *Nature medicine*, 31(3): 932–942.
- Mazeika, M.; Phan, L.; Yin, X.; Zou, A.; Wang, Z.; Mu, N.; Sakhaee, E.; Li, N.; Basart, S.; Li, B.; et al. 2024. Harmbench: A standardized evaluation framework for automated red teaming and robust refusal. *arXiv preprint arXiv:2402.04249*.
- Meta AI. 2024. LLaMA 3 Model Card. https://github.com/meta-llama/llama3/blob/main/MODEL_CARD.md. Accessed: 2025-07-31.
- OpenAI. 2024. GPT-4o Technical Report. <https://openai.com/index/gpt-4o>. Accessed: 2025-08-01.
- Phute, M.; Helbling, A.; Hull, M.; Peng, S.; Szyller, S.; Cornelius, C.; and Chau, D. H. 2023. Llm self defense: By self examination, llms know they are being tricked. *arXiv preprint arXiv:2308.07308*.
- Qi, X.; Zeng, Y.; Xie, T.; Chen, P.-Y.; Jia, R.; Mittal, P.; and Henderson, P. 2023. Fine-tuning aligned language models

compromises safety, even when users do not intend to! *arXiv preprint arXiv:2310.03693*.

Rosati, D.; Wehner, J.; Williams, K.; Bartoszcze, L.; Atanasov, D.; Gonzales, R.; Majumdar, S.; Maple, C.; Sajjad, H.; and Rudzicz, F. 2024. Representation noising effectively prevents harmful fine-tuning on llms. *CoRR*.

Shao, Z.; Wang, P.; Zhu, Q.; Xu, R.; Song, J.; Bi, X.; Zhang, H.; Zhang, M.; Li, Y.; Wu, Y.; et al. 2024. Deepseekmath: Pushing the limits of mathematical reasoning in open language models. *arXiv preprint arXiv:2402.03300*.

Shen, G.; Zhao, D.; Dong, Y.; He, X.; and Zeng, Y. 2024. Jailbreak antidote: Runtime safety-utility balance via sparse representation adjustment in large language models. *arXiv preprint arXiv:2410.02298*.

Stiennon, N.; Krause, A.; Laskin, M.; Luan, Y.; Schulman, J.; and Christiano, P. 2020. Learning to Summarize with Human Feedback. *arXiv preprint arXiv:2009.01325*.

Tamirisa, R.; Bharathi, B.; Phan, L.; Zhou, A.; Gatti, A.; Suresh, T.; Lin, M.; Wang, J.; Wang, R.; Arel, R.; et al. 2024. Tamper-resistant safeguards for open-weight llms. *arXiv preprint arXiv:2408.00761*.

Taori, R.; Gulrajani, I.; Zhang, T.; Dubois, Y.; Li, X.; Guestrin, C.; Liang, P.; and Hashimoto, T. B. 2023. Stanford alpaca: An instruction-following llama model.

Wei, B.; Huang, K.; Huang, Y.; Xie, T.; Qi, X.; Xia, M.; Mittal, P.; Wang, M.; and Henderson, P. 2024. Assessing the brittleness of safety alignment via pruning and low-rank modifications. *arXiv preprint arXiv:2402.05162*.

Wei, Z.; Wang, Y.; Li, A.; Mo, Y.; and Wang, Y. 2023. Jailbreak and guard aligned language models with only few in-context demonstrations. *arXiv preprint arXiv:2310.06387*.

Xie, Y.; Yi, J.; Shao, J.; Curl, J.; Lyu, L.; Chen, Q.; Xie, X.; and Wu, F. 2023. Defending chatgpt against jailbreak attack via self-reminders. *Nature Machine Intelligence*, 5(12): 1486–1496.

y Arcas, B. A. 2022. Do large language models understand us? *Daedalus*, 151(2): 183–197.

Yang, A.; Yang, B.; Zhang, B.; Hui, B.; Zheng, B.; Yu, B.; Li, C.; Zhang, . Z.; and Qiu, Z. 2024. Qwen2.5 Technical Report. ArXiv:2412.15115.

Yi, X.; Zheng, S.; Wang, L.; de Melo, G.; Wang, X.; and He, L. 2025. Nlsr: Neuron-level safety realignment of large language models against harmful fine-tuning. In *Proceedings of the AAAI Conference on Artificial Intelligence*, volume 39, 25706–25714.

Zhang, Z.; Yang, J.; Ke, P.; Mi, F.; Wang, H.; and Huang, M. 2023. Defending large language models against jailbreaking attacks through goal prioritization. *arXiv preprint arXiv:2311.09096*.

Zhu, M.; Yang, L.; Wei, Y.; Zhang, N.; and Zhang, Y. 2024. Locking down the finetuned llms safety. *arXiv preprint arXiv:2410.10343*.

Zong, Y.; Bohdal, O.; Yu, T.; Yang, Y.; and Hospedales, T. 2024. Safety fine-tuning at (almost) no cost: A baseline for vision large language models. *arXiv preprint arXiv:2402.02207*.